Impact Assessment of Ammonia Emissions on Inorganic Aerosols in East China Using Response Surface Modeling Technique

ARTICLE *in* ENVIRONMENTAL SCIENCE & TECHNOLOGY · SEPTEMBER 2011

Impact Factor: 5.33 · DOI: 10.1021/es2022347 · Source: PubMed

Shuxiao Wang
Tsinghua University
145 PUBLICATIONS **2,778** CITATIONS
SEE PROFILE

Jia Xing
United States Environmental Protection Age…
39 PUBLICATIONS **836** CITATIONS
SEE PROFILE

Joshua S Fu
University of Tennessee
162 PUBLICATIONS **2,249** CITATIONS
SEE PROFILE

Environmental Science & Technology

ARTICLE

pubs.acs.org/est

Impact Assessment of Ammonia Emissions on Inorganic Aerosols in East China Using Response Surface Modeling Technique

Shuxiao Wang,*,† Jia Xing,† Carey Jang,‡ Yun Zhu,§ Joshua S. Fu,∥ and Jiming Hao†

†School of Environment, and State Key Joint Laboratory of Environment Simulation and Pollution Control, Tsinghua University, Beijing 100084, P. R. China

‡U.S. Environmental Protection Agency, Research Triangle Park, North Carolina 27711, United States

§School of Environmental Science and Engineering, South China University of Technology, Guangzhou 510006, P. R. China

∥Department of Civil and Environmental Engineering, University of Tennessee, Knoxville, Tennessee 37996, United States

Supporting Information

ABSTRACT: Ammonia (NH_3) is one important precursor of inorganic fine particles; however, knowledge of the impacts of NH_3 emissions on aerosol formation in China is very limited. In this study, we have developed China's NH_3 emission inventory for 2005 and applied the Response Surface Modeling (RSM) technique upon a widely used regional air quality model, the Community Multi-Scale Air Quality Model (CMAQ). The purpose was to analyze the impacts of NH_3 emissions on fine particles for January, April, July, and October over east China, especially those most developed regions including the North China Plain (NCP), Yangtze River delta (YRD), and the Pearl River delta (PRD). The results indicate that NH_3 emissions contribute to 8−11% of $PM_{2.5}$ concentrations in these three regions, comparable with the contributions of SO_2 (9−11%) and NO_x (5−11%) emissions. However, NH_3, SO_2, and NO_x emissions present significant nonlinear impacts; the $PM_{2.5}$ responses to their emissions increase when more control efforts are taken mainly because of the transition between NH_3-rich and NH_3-poor conditions. Nitrate aerosol (NO_3^-) concentration is more sensitive to NO_x emissions in NCP and YRD because of the abundant NH_3 emissions in the two regions, but it is equally or even more sensitive to NH_3 emissions in the PRD. In high NO_3^- pollution areas such as NCP and YRD, NH_3 is sufficiently abundant to neutralize extra nitric acid produced by an additional 25% of NO_x emissions. The 90% increase of NH_3 emissions during 1990−2005 resulted in about 50−60% increases of NO_3^- and SO_4^{2-} aerosol concentrations. If no control measures are taken for NH_3 emissions, NO_3^- will be further enhanced in the future. Control of NH_3 emissions in winter, spring, and fall will benefit $PM_{2.5}$ reduction for most regions. However, to improve regional air quality and avoid exacerbating the acidity of aerosols, a more effective pathway is to adopt a multipollutant strategy to control NH_3 emissions in parallel with current SO_2 and NO_x controls in China.

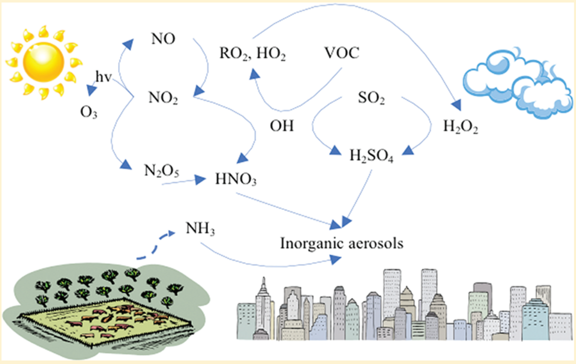

INTRODUCTION

The importance of ammonia (NH_3) in contributing to secondary inorganic aerosols (SIA, i.e., sulfate (SO_4^{2-}), nitrate (NO_3^-), and ammonium (NH_4^+)) has been well documented in recent studies. Excess NH_3 provides a weak base, which allows a larger aqueous uptake of sulfur dioxide (SO_2) to be oxidized and, at the same time, also affects the effective cloud SO_2 oxidation rate due to strong pH-dependent oxidation by ozone (O_3).[1,2] In the presence of NH_3, NO_3^- is formed by the gas-to-particle conversion process from nitric acid (HNO_3) which was first produced through a photochemical reaction as nitrogen dioxide (NO_2) and hydroxyl radical (•OH). Multisensitivity studies for European countries and the United States[2−9] have been conducted using air quality models (AQMs) to explore the response of inorganic fine particles to emission changes of SO_2, nitrogen oxides ($NO_x = NO + NO_2$), NH_3, or nonmethane volatile organic compounds (NMVOC). Derwent et al.[9] used a moving air parcel trajectory model to estimate the mass concentrations of PM components for a rural location in the southern UK, and found that PM mass concentrations are nonlinear with PM precursor emissions, and suggested that abatement of NH_3 emissions should be considered to obtain the largest $PM_{2.5}$ reduction. Tsimpidi et al.[2] applied a three-dimensional chemical transport model (PMCAMx) to investigate the changes in $PM_{2.5}$ concentrations responding to changes of SO_2 and NH_3 emissions in the eastern United States, and indicated that coupled reductions of SO_2 and NH_3 emissions are more effective than the

Received: June 30, 2011
Accepted: September 22, 2011
Revised: September 8, 2011
Published: September 22, 2011

dx.doi.org/10.1021/es2022347 | Environ. Sci. Technol. 2011, 45, 9293–9300

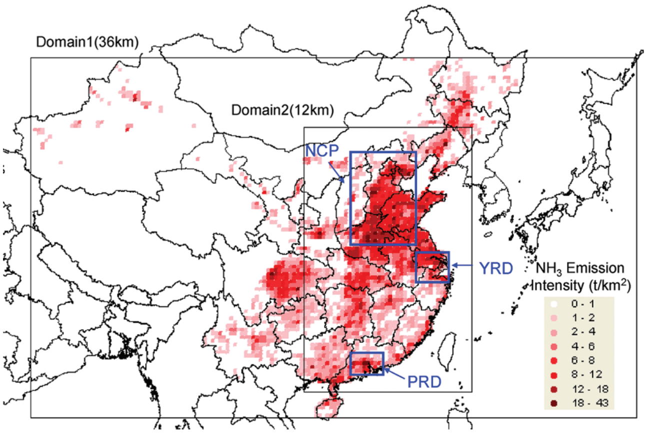

Figure 1. Map of the CMAQ/RSM modeling domain and spatial distributions of NH_3 emissions.

control of individual pollutants. Pinder et al.[6] conducted a series of PMCAMx simulations to estimate the cost-effectiveness and uncertainty of NH_3 emission reductions on inorganic aerosols in the eastern United States and found that many currently available NH_3 control technologies were cost-effective compared to SO_2 and NO_x.

China, as the most populated country in the world, has significant agricultural activities which release large amounts of NH_3 to the atmosphere. Enhanced concentrations of NH_3 over the Beijing area in northeast China have been first detected in space-based nadir viewing measurements that penetrate into the lower atmosphere.[10] The North China Plain (NCP), as shown in Figure 1, is one of the areas with the highest NH_3 column density retrieved from infrared satellite observations.[11] National NH_3 emissions in China are estimated to be 12−14 Tg for year 2000 and 13−16 Tg for year 2005,[12−14] and account for 30−55% of total Asia NH_3 emissions.[12,15,16] SO_2 emissions have become better controlled in China.[17] National emissions of SO_2 were required by the government to be reduced 10% by 2010 compared to the level in 2005. However, such reduction of SO_2 may adversely affect $PM_{2.5}$, because it will lead to an increase in aerosol nitrate in the regions where air quality is more acidic.[5,18,19] Additionally, in terms of acidification effects, Zhao et al.[20] indicated that the benefits of SO_2 reductions by 10% in China during 2005 to 2010 would almost be negated by the increase of NO_x and NH_3 emissions. Xing et al.[18] suggested NH_3 emission control should be considered to reduce the total nitrogen deposition in the future.

Undoubtedly, NH_3 is one of the most important pollutants which should receive attention; however, modeling studies to understand the impacts of NH_3 emission on fine particles in China are quite limited. In this paper, we conducted 3-D air quality simulations in conjunction with the Response Surface Modeling (RSM) technique to investigate sensitivities of the PM components to changes of their precursor emissions, including SO_2, NO_x, NH_3, NMVOC, and primary particles, in east China. Nonlinear impacts of NH_3 emissions on SIA have been evaluated, and a more effective NH_3 emission control pathway is recommended.

METHODOLOGY

The processes involved are the establishment of emission inventories, selection of air quality modeling domain and configuration, development, and validation of the emission control/air quality response prediction using RSM methodology.

Emission Inventory. Emissions of SO_2, NO_x, PM_{10}, $PM_{2.5}$, black carbon (BC), organic carbon (OC), NH_3, and NMVOC were calculated based on the framework of the GAINS-Asia model.[21] The general method and some improvements used to develop the China regional emission inventory are described in our previous papers.[22]

In 2005, NH_3 emissions from livestock farming, N-fertilizer application, N-fertilizer production, and human excreta are estimated to be 7.16, 8.35, 0.17, and 0.87 Tg, respectively. The first two are the most important NH_3 contributors; they account for 43% and 50% of total emissions, respectively. Urea, ammonium bicarbonate (ABC), and other fertilizers account for 56%, 22%, and 22% of the N-fertilizer used in China. The consumption of N-fertilizer has been increasing in the past 15 years. In 2010, the consumption of ammonia fertilizer was 26.4% higher than that in 2005. Large variations presented in the geographical distribution are shown in Figure 1. The North China Plain, including Henan, Shandong, Hebei, and Jiangsu Provinces, contribute approximately 33% of national emissions, with an emission intensity as high as 9.0 t km^{-2}, 4 times above the national average level (i.e., 1.7 t km^{-2}). NH_3 emissions have strong seasonal variations since the related agricultural activities and emission factors (i.e., N-volatilization rate) are significantly affected by the meteorological conditions.[12,14,23,24] Highest NH_3 emissions occur during June−August because of more favorable meteorological conditions (i.e., higher temperature) for NH_3 volatilization and intensive agricultural activities. In this study, the monthly NH_3 emissions in January, April, July, and October are estimated as 2.9%, 4.2%, 18.3%, and 7.5% of annual emissions, respectively.

MM5/CMAQ Modeling. The air quality model used in this study is the Model-3/Community Multiscale Air Quality (CMAQ) modeling system (ver. 4.7), developed by U.S. EPA,[25] which has been tested, evaluated, and applied in China.[26−31] A one-way nested technique is employed in this study. Modeling domain 1 covers almost all of China with a 36 × 36 km horizontal grid resolution and generates the boundary conditions for nested domain at 12 × 12 km resolution over East China. The three most developed regions, North China Plain (NCP), Yangtze River delta (YRD), and Pearl River delta (PRD), have been chosen as the target areas, as shown in Figure 1 and Table S1. The target period is January, April, July, and October in 2005. A complete description of CMAQ configuration, meteorological, emission, and initial and boundary condition inputs used for this analysis are described in Xing et al.[18,33] The Aerosol Optical Depth (AOD), NO_2 and SO_2 column density, as well as the ground concentrations of SO_2, NO_2, PM_{10}, $PM_{2.5}$, and its chemical components simulated by this modeling system have been validated through comparison with observations of satellite retrievals and surface monitoring data.

Response Surface Modeling (RSM) Technique. A real-time emission control/air quality response tool, i.e., RSM, was developed at the U.S. EPA and applied to a number of air quality policy analyses and assessments.[32] RSM uses advanced statistical techniques to characterize the relationships between model outputs (i.e., air quality responses) and input parameters (i.e., emission changes) in a highly efficient manner. Table 1 gives the sampling method and numbers of simulations used in this RSM application. Following the principle of RSM development as discussed in our previous paper,[33] the responses of PM concentrations to

Table 1. Sample Methods and Key Parameters Involved during PM RSM Development

RSM case	variable number	sample method	sample number
LHS-30-a	total-NO_x, total-SO_2	Latin hypercube sampling	30
LHS-30-b	total-NO_x, total-NH_3	Latin hypercube sampling	30
LHS-30-c	total-SO_2, total-NH_3	Latin hypercube sampling	30
LHS-30-d	total-NO_x, total-NMVOC	Latin hypercube sampling	30
HSS-100	total-NO_x, SO_2, NH_3, NMVOC, and PM	Hammersley quasi-random sequence sample	100

the changes of the total emissions of SO_2, NO_x, NH_3, NMVOC, and PM over east China have been calculated. We define "emission ratios" as the ratio of the changed emissions compared to the baseline emissions. The emissions of each pollutant change from 0 to 200%, which means the emission ratios are from 0 to 2. We used 100 random emission control scenarios generated by Hammersley quasi-random Sequence Sample (HSS) method to establish the emission-based prediction model (HSS-100). In this study, RSM surface (emissions control and corresponding concentration change) prediction system is statistically generalized by MPerK (MATLAB Parametric Empirical Kriging) program followed Maximum Likelihood Estimation—Experimental Best Linear Unbiased Predictors (MLE-EBLUPs).[34] Such control/response prediction system (i.e., HSS-100) has been validated through "leave-one-out cross validation" (LOOCV) (see Table S2), "out of sample" validation (see Table S3) and 2-D isopleths validation (see Figures S1 and S2). These results indicate that the HSS-100 predictions have good accuracy compared with CMAQ simulations. The stability of RSM with high dimensions (i.e., HSS-100) has been confirmed through its comparison with the one with low dimensions (i.e., LHS-30).

RESULTS AND DISCUSSION

$PM_{2.5}$ Sensitivity to NH_3 Emissions. Following other sensitivity studies,[35,36] we defined the $PM_{2.5}$ sensitivity as the change ratio of $PM_{2.5}$ concentration change to the change ratio of emissions, to evaluate the control effects of each pollutant,

$$S_a^X = \frac{\Delta C/C^*}{\Delta E_X/E_X^*} = \frac{(C^* - C_a)/C^*}{1-a} \tag{1}$$

where S_a^X is the $PM_{2.5}$ sensitivity to pollutant X (i.e., SO_2, NO_x, NH_3, NMVOC, and PM) at its emission ratio a; C_a is the concentration of $PM_{2.5}$ when the emission ratio of X is a; C^* is the baseline concentration of $PM_{2.5}$ (when emission ratio of X is 1).

Figure 2 gives the comparison of $PM_{2.5}$ sensitivities to the emissions of each pollutant (i.e., SO_2, NO_x, NH_3, NMVOC, and PM) in the three target regions. The SIA accounts for about 20−50% of $PM_{2.5}$ concentrations in three regions, which is consistent with observations.[37] The $PM_{2.5}$ sensitivities to PM emissions are about the same in various control levels. However, NH_3, SO_2, and NO_x present significant nonlinear impacts; the $PM_{2.5}$ sensitivities to their emissions get larger when more control efforts are taken, because of the transition between NH_3-rich and NH_3-poor conditions, the transition between NO_x-limited and VOC-limited for ozone chemistry regimes and other thermodynamic effect and etc. The $PM_{2.5}$ response to NH_3 emissions is comparable with that of SO_2 and NO_x, and it is larger under higher control levels. Under 50% control level, NH_3, NO_x, and SO_2 emissions reduce 7.9%, 10.8%, and 10.4% of $PM_{2.5}$ concentrations in NCP; 10.7%, 7.7%, and 8.9% in YRD; 9.9%, 5.2%, and 10.8% in PRD; and 10.7%, 10.2%, and 11.4% in east China.

Nonlinear Impacts of NH_3 Emission on SO_4^{2-} and NO_3^- Aerosol. The reaction mechanism of atmospheric chemistry is given in Figure S3. Using the Beijing urban site as an example, the nonlinear response of SO_4^{2-} and NO_3^- aerosol concentrations to the emission changes of precursors, is given in Figure 3.

For SO_4^{2-} concentration, the dominating contributor is SO_2 emissions (Figure 3a, c). NH_3 emissions slightly enhance the SO_4^{2-} concentrations under NH_3-poor condition, because NH_3 provides a weak base condition to uptake more SO_2 and also enhances the cloud SO_2 oxidation rate by O_3. But no effects are found under NH_3-rich condition for both January and July (Figure 3c). Lower NO_x emissions (an emission ratio of 0.2−0.4 in January and 0.7−0.9 in July, higher in summer due to stronger atmospheric oxidation capacity than in winter) and suitable NO_x/NMVOC ratios benefit SO_4^{2-} generation (Figure 3b, d). The hydroxyl radical is the key reactive species in both homogeneous (SO_2 + •OH) or aqueous-phase paths of SO_4^{2-} formation. Both NO_x and NMVOC could be involved in •OH removals during the generation of NO_3^- and RO_2/HO_2, therefore suitable NO_x/NMVOC ratios will enhance the generation of ozone, the major source of the hydroxyl radical. In NO_x-rich conditions, the SO_4^{2-} sensitivity to NO_x emissions is negative. The results are opposite in NO_x- poor conditions.

For NO_3^- concentration, NO_x emissions are the dominating contributor. However, NH_3 emissions are very important under NH_3-poor conditions (as shown in Figure 3b), because NH_3 reacts preferentially with H_2SO_4 instead of HNO_3. The sensitivities of NO_3^- concentration to NO_x and NH_3 emissions (under baseline, i.e., emission ratio =1) are relatively larger in summer than those in winter, because NO_3^- is very volatile in the summer (due to high temperature) and, thus, the equilibrium moves dominantly toward the gas-phase HNO_3 instead of particle-phase NH_4NO_3. SO_2 emissions slightly benefit NO_3^- formation under NH_3-rich conditions, especially at lower SO_2 emissions level (Figure 3c). This is caused by the thermodynamic effect.[2] The increase of NH_4^+ and SO_4^{2-} ions will decrease the NH_4NO_3 equilibrium constant, shifting its partitioning toward the particulate phase.[38] However, when NH_3 is insufficient, SO_2 emissions inhibit NO_3^- formation due to its competition with NH_3. NMVOC emission slightly contributes NO_3^- pollution under NO_x-rich condition in both January and July, and NO_x emission slightly inhibits NO_3^- formation under NO_x-rich condition in January (Figure 3d).

Identification of NH_3-Rich/-Poor Condition. Indicators for PM chemistry such as the degree of sulfate neutralization (DSN), gas ratio (GR), and adjusted gas ratio (AdjGR) could be used to identify the NH_3-poor, -neutral, or -rich condition, then to

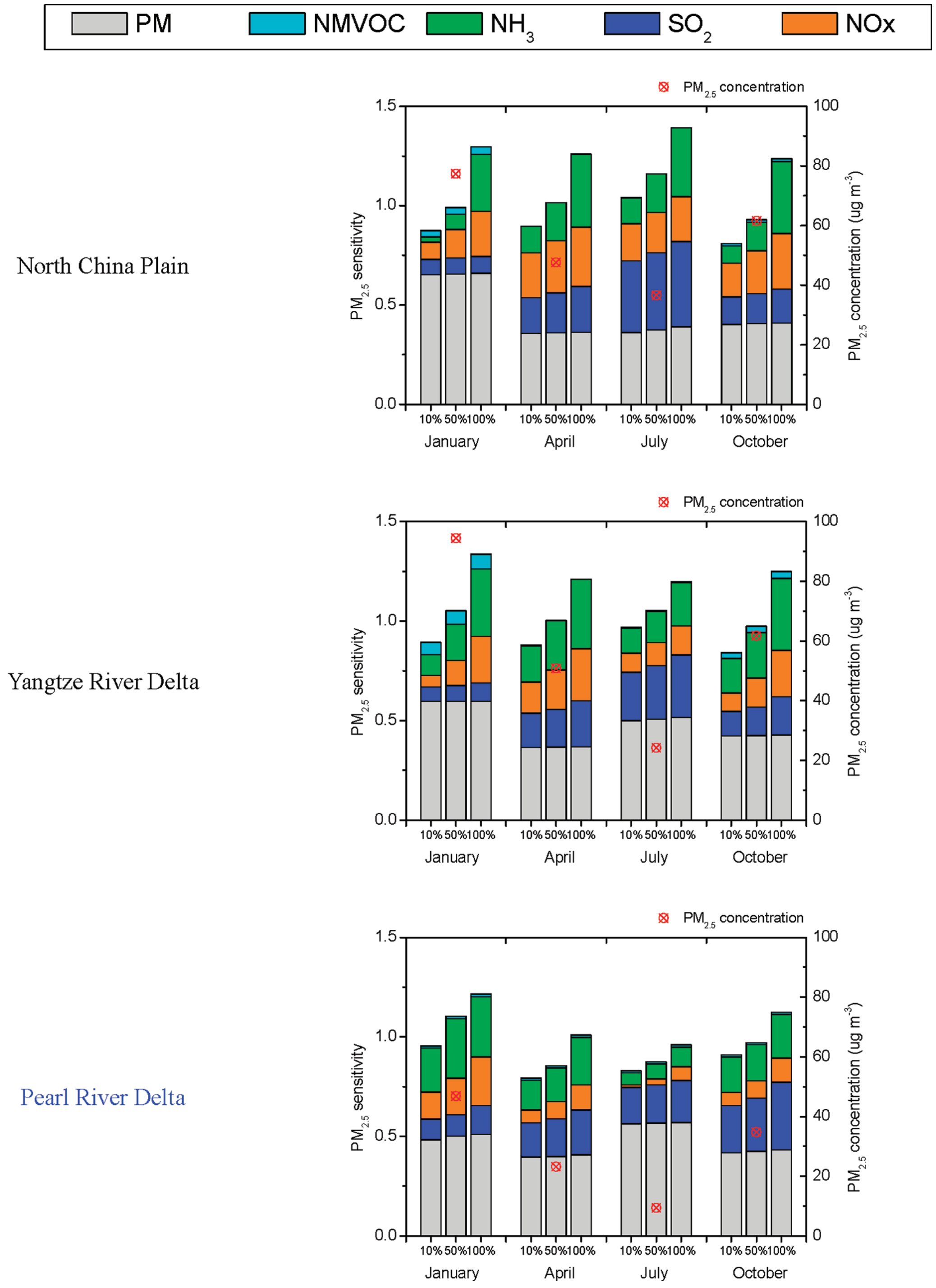

Figure 2. $PM_{2.5}$ concentration sensitivity to the stepped control of individual pollutants ($PM_{2.5}$ sensitivity = change ratio of $PM_{2.5}$/change ratio of emission; all values are monthly average in January, April, July, and October in 2005).

determine the sensitivity of NO_3^- to precursors' emissions.[39] Their definitions are given as follows:

$$\mathrm{DSN} = \frac{[\mathrm{NH}_4^+] - [\mathrm{NO}_3^-]}{[\mathrm{SO}_4^-]} \tag{2}$$

$$\mathrm{GR} = \frac{[\mathrm{TA}] - 2 \times [\mathrm{TS}]}{[\mathrm{TN}]} = \frac{([\mathrm{NH}_3] + [\mathrm{NH}_4^+]) - 2 \times [\mathrm{SO}_4^{2-}]}{[\mathrm{NO}_3^-] + [\mathrm{HNO}_3]} \tag{3}$$

$$\mathrm{AdjGR} = \frac{[\mathrm{TA}] - \mathrm{DSN} \times [\mathrm{TS}]}{[\mathrm{TN}]} = \frac{[\mathrm{NH}_3] + [\mathrm{NO}_3^-]}{[\mathrm{NO}_3^-] + [\mathrm{HNO}_3]} \tag{4}$$

where [TA], [TN], and [TS] are the total molar concentration of ammonia ($[NH_3] + [NH_4^+]$), nitrate ($[NO_3^-] + [HNO_3]$), and sulfate ($[SO_4^{2-}]$), respectively.

From RSM results, not only the NH_3-rich/-poor condition under baseline scenario but also that under certain emission

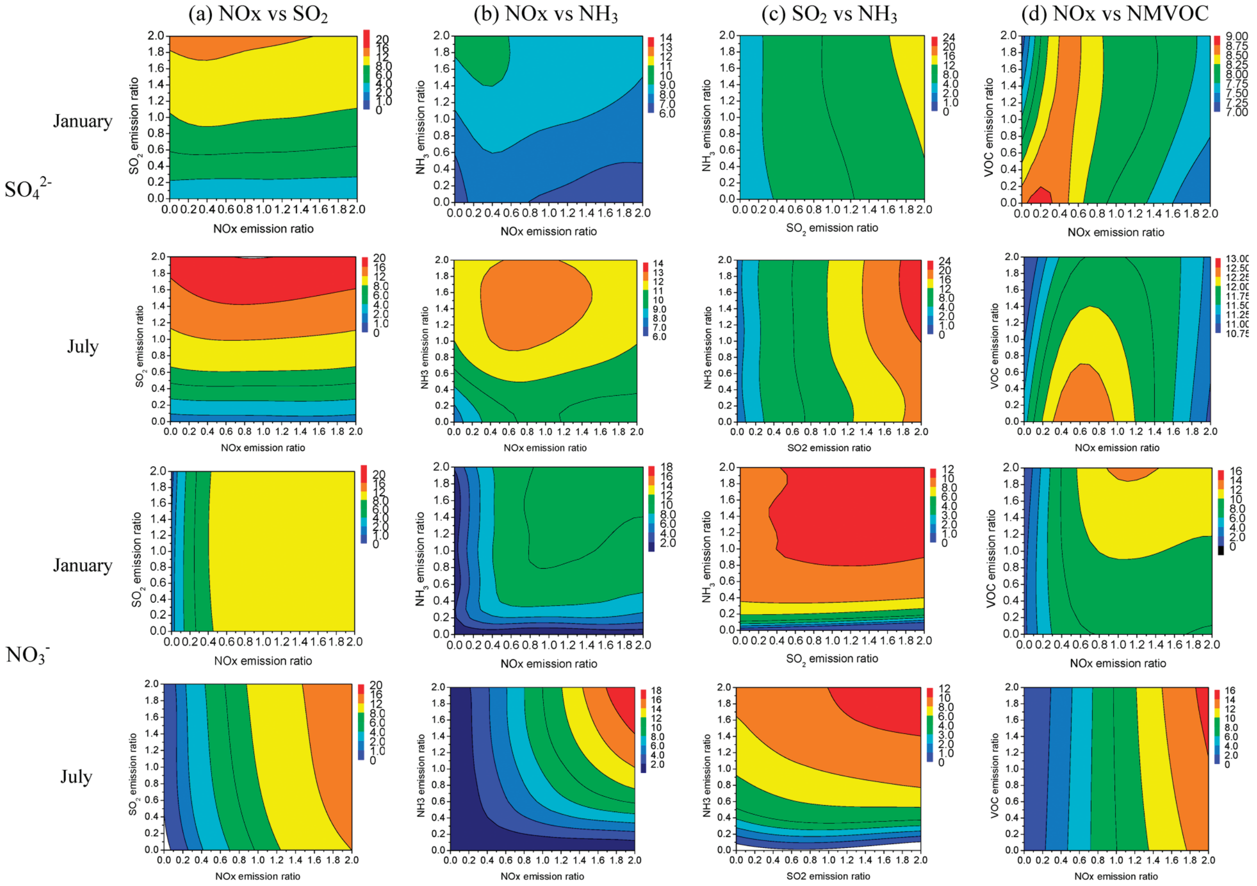

(a) NOx vs SO2 (b) NOx vs NH3 (c) SO2 vs NH3 (d) NOx vs NMVOC

Figure 3. 2-D Isopleths of SO_4^{2-} and NO_3^- response to the emission changes of NO_x, SO_2, NH_3, and NMVOC in Beijing, monthly average, 2005 ($\mu g/m^3$).

control scenarios can be determined.[30] The NH_3-poor condition means the total available ammonia (gaseous ammonia + aerosol phase ammonium) is insufficient to charge-balance difference the remaining of other anions and cations,[40] with the result that small perturbations in the ammonia emissions may have a significant effect on particle mass.[41] Based on this principle, we defined an indicator—"Flex Ratio (FR)"—to identify the NH_3-poor/-rich condition. As shown in Figure S4, under baseline NO_x emissions (i.e., NO_x emission ratio = 1), along with the decrease of NH_3 emission ratio from 2.0 to 0, the NO_3^- slightly increases at first, but it gets sharply increased after the transition point (i.e., Flex Ratio). In the isopleths of NO_3^- response to NO_x/NH_3 emission changes predicted by RSM, the Flex Ratio is defined as the NH_3 emission ratio at the flex NO_3^- concentrations under baseline NO_x emissions (see Figure S4). When the FR is larger than the current NH_3 emission ratio (in baseline = 1), the sensitivity of the NO_3^- concentration to NH_3 emissions is more than that to NO_x emissions, which indicate NH_3-poor condition (see Table S4). In contrast, when the FR is less than 1, the NO_3^- concentration is more sensitive to NO_x emissions instead of NH_3 emissions, which indicates a NH_3-rich condition, and the value (1 − FR) reflects the ratio of free NH_3 which could neutralize extra nitric acid produced by additional increases of NO_x emissions.

The spatial distributions of NO_3^- concentrations and GR are given in Figure S5. NO_3^- concentrations are found higher in January and lower in July, since higher temperature benefits NO_3^- evaporation and stronger atmospheric oxidation capacity favors converting S(IV) to S(VI), then enhancing the NH_3 competition between SO_4^{2-} and NO_3^- in July. Values of GR indicate NH_3-rich, neutral, and poor conditions.[39] The spatial distributions of GR value suggest that most of the polluted areas are located in NH_3-rich conditions in all months (i.e., GR > 1). The FR over east China is shown in Figure 4. The FR derived from RSM gives consistent results, and the FR values in heavy NO_3^- pollution areas are mainly below 0.8. On an average annual basis, NCP and YRD are mainly located in NH_3-rich conditions (FR is 0.6−0.7 and 0.8−1.0, respectively), therefore NO_3^- is more sensitive to NO_x emissions, but PRD is located in NH_3-poor conditions (FR is 1.0−1.5) and NO_3^- in PRD is more sensitive to NH_3 emissions. The FR is around 0.8 in high NO_3^- areas, indicating NH_3 is sufficiently abundant to satisfy an additional 25% (= 1/0.8 − 1) increase of NO_x emissions to generate NO_3^-.

Impacts of NH_3 Emission Increase on SO_4^{2-} and NO_3^- Aerosols. Previous studies on the emission trends in China indicate the NH_3 emissions have been growing along with other precursors. According to these results, the emission trends for each pollutant during 1990−2005 could be fitted by parameterized quadratic functions, as shown in Figure 5a. NO_x is the fastest growing pollutant, increasing over 100% from 1990 to 2005. SO_2 emissions have increased by 30% during the same period. The NH_3 and NMVOC emissions in 2005 are about 90% increased from that in 1990.

The growth trends of SO_4^{2-} and NO_3^- concentrations driven by the increases of the emissions during 1990−2005 have been calculated by RSM. The results are given in Figure 5

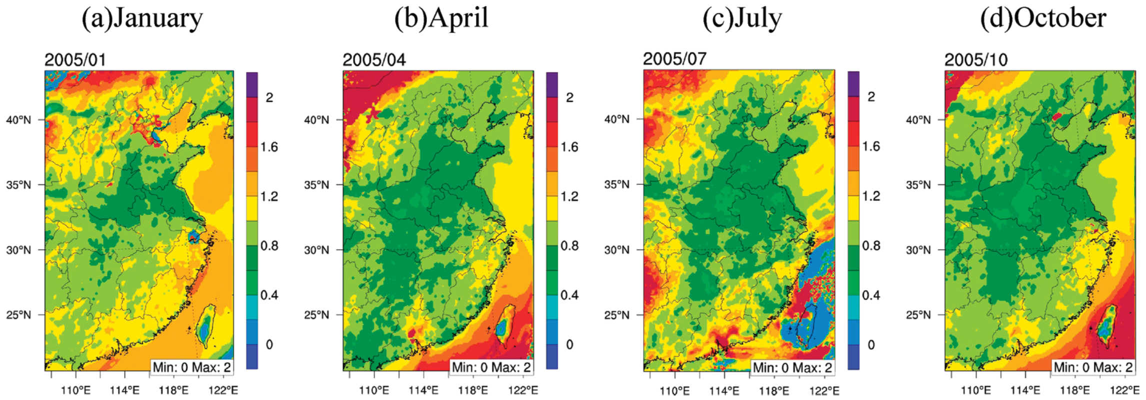

Figure 4. Flex ratio in January, April, July, and October, 2005 (FR < 1 suggests NH_3-rich condition; FR > 1 suggests NH_3-poor condition).

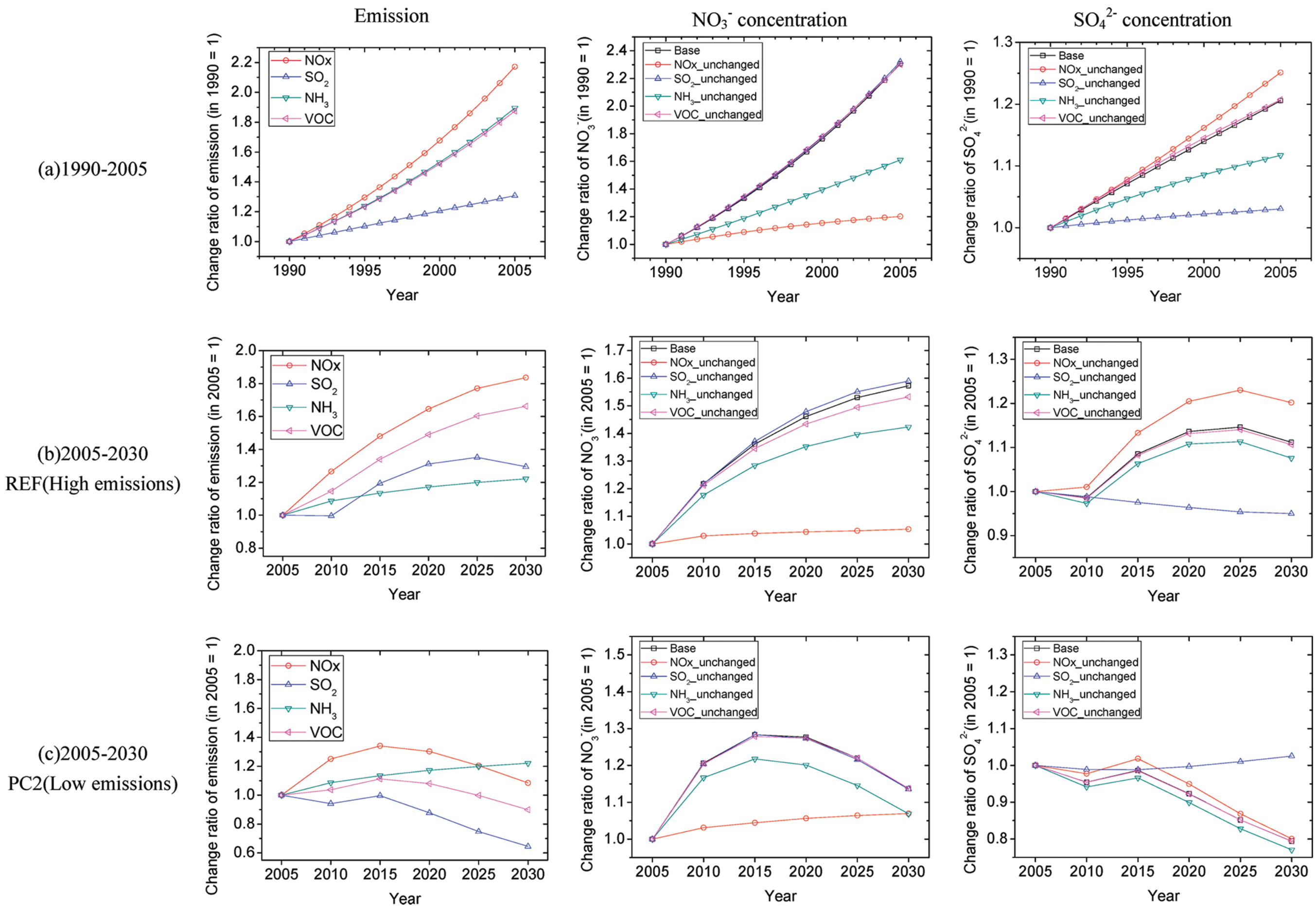

Figure 5. Historical and future growth of emissions impacts on SO_4^{2-} and NO_3^- (average of 4 months, in east China).

(in a 4-month average). As seen in Figure 5, the base scenario reflects the impacts of all five pollutants emission simultaneous changes with SO_4^{2-} and NO_3^- concentration. In addition, a series of hypothetical scenarios has been conducted to evaluate the impacts of each pollutant emission change on SO_4^{2-} and NO_3^- concentrations. In each hypothetical scenario, one pollutant is held at the 1990 level (i.e., no increases during 1990–2005) and the rest are kept the same as the base scenario. In the baseline, the NO_3^- and SO_4^{2-} concentrations increase by 150% and 20%, respectively. It is obvious that the growth of NO_x and SO_2 emissions are the dominant factor to enhance NO_3^- and SO_4^{2-}, respectively. Significant impacts could also be seen from the growth of NH_3 emissions. About 50–60% increases of NO_3^- and SO_4^{2-} are caused by the growth of NH_3 emissions. The growths of NMVOC and SO_2 emissions have no significant impacts on NO_3^-, while the growth of NO_x hasnegative impacts on SO_4^{2-} formation, possibly due to its influence on •OH as discussed in the previous section, especially during wintertime.

Emissions of air pollutants and their projections have been changing significantly in recent years. The satellite data have shown that NO_2 increase in East Asia has been growing much faster than previous projections. Therefore, it is important to understand how China's air pollutant emission change will affect the regional air quality in the future. Alternative scenarios for future SO_2, NO_x, and NMVOC emissions [18] were developed using forecasts of energy consumption and emission control strategies based on emissions in 2005, and on recent development plans for key industries in China, as shown in Figure 5b and c. In the reference scenario, which is based on the current control legislations and implementation status, i.e., REF scenario, the emissions of all pollutants are increasing from 2005 to 2030. In 2030, NO_3^- and SO_4^{2-} will increase significantly, by 50% and 10%, respectively. In 2030, the NH_3 emissions will increase by 20%, which may cause 15% and 4% increase of NO_3^- and SO_4^{2-}, respectively. In the policy scenario, which is based on the improvement of energy efficiencies and strict environmental legislation, i.e., PC2 scenario, though NO_x emissions will be better controlled in 2030, the increase of NH_3 emissions will enhance NO_3^- by 10%. The decrease of SO_2 emissions leads to significant reduction of SO_4^{2-}, while the growth of NH_3 will slightly improve SO_4^{2-} by 2%. This implies future potential control of NH_3 is important, especially for NO_3^- reduction.

NH_3 Impacts on the Acidity of Aerosols. The major concern about the potential negative impacts of NH_3 control is the enhancement of aerosol acidity. In this study, we select the DSN as the indicator of the acidity of aerosols. When the DSN is less than 2, SO_4^{2-} is insufficiently neutralized and the aerosol is more likely to be acid. The NH_3 emissions level resulting in DSN less than 2 are calculated from RSM. Its spatial distributions over four months are given in Figure S6. High NH_3 emissions are beneficial to the formation of NO_3^-. Over the polluted areas such as NCP and YRD which have the highest NH_3 emission intensities,[14] the values are 0.8−1 in January, April, and October, but higher than 1 in July. This indicates the acidity of aerosols is more sensitive to NH_3 emissions in summer than in other seasons, mainly because of the high evaporation of NO_3^- in summer and the stronger atmospheric oxidation capacity which converts S(IV) to S(VI) and enhances the NH_3 competition between SO_4^{2-} and NO_3^- in July. Therefore, the acidity of aerosols is more sensitive to NH_3 emissions in the summer than in other seasons.

ASSOCIATED CONTENT

Supporting Information. This information is available free of charge via the Internet at http://pubs.acs.org/.

AUTHOR INFORMATION

Corresponding Author

*Phone: +86-10-62771466; fax: +86-10-62773650; e-mail: shxwang@tsinghua.edu.cn.

ACKNOWLEDGMENT

The study was financially supported by Natural Science Foundation of China (20921140409), MEP's Special Funds for Research on Public Welfares (201009001), and the U.S. EPA. We thank Dr. Thomas J. Santner and Dr. Gang Han at The Ohio State University for their help using the MperK program and Satoru Chatani from Toyota Central R&D Laboratories for aid with emission processing. We appreciate that Dr. Chuck Freed helped improve the language of the paper.

REFERENCES

(1) Makar, P. A.; Moran, M. D.; Zheng, Q.; Cousineau, S.; Sassi, M.; Duhamel, A.; Besner, M.; Davignon, D.; Crevier, L.-P.; Bouchet, V. S. Modelling the impacts of ammonia emissions reductions on North American air quality. *Atmos. Chem. Phys.* **2009**, *9*, 7183–7212, DOI: 10.5194/acp-9-7183-2009.

(2) Tsimpidi, A. P.; Karydis, V. A.; Pandis, S. N. Response of Inorganic Fine Particulate Matter to Emission Changes of Sulfur Dioxide and Ammonia: The Eastern United States as a Case Study. *J. Air Waste Manage. Assoc.* **2007**, *57*, 1489–1498, DOI: 10.3155/1047-3289.57.12.1489.

(3) Nguyen, K.; Dabdub, D. NO_x and VOC Control and Its Effects on the Formation of Aerosols. *Aerosol Sci. Technol.* **2002**, *36*, 560–572.

(4) Mueller, S. F.; Bailey, E. M.; Kelsoe, J. J. Geographic Sensitivity of Fine Particle Mass to Emissions of SO2 and NO_x. *Environ. Sci. Technol.* **2004**, *38*, 570–580.

(5) Blanchard, C. L.; Tanenbaum, S.; Hidy, G. M. Effects of Sulfur Dioxide and Oxides of Nitrogen Emission Reductions on Fine Particulate Matter Mass Concentrations: Regional Comparisons. *J. Air Waste Manage. Assoc.* **2007**, *57*, 1337–1350, DOI: 10.3155/1047-3289.57.11.1337.

(6) Pinder, R. W.; Adams, P. J.; Pandis, S. N. Ammonia Emission Controls as a Cost-Effective Strategy for Reducing Atmospheric Particulate Matter in the Eastern United States. *Environ. Sci. Technol.* **2007**, *41*, 380–386.

(7) Tsimpidi, A. P.; Karydis, V. A.; Pandis, S. N. Response of Fine Particulate Matter to Emission Changes of Oxides of Nitrogen and Anthropogenic Volatile Organic Compounds in the Eastern United States. *J. Air Waste Manage. Assoc.* **2008**, *58*, 1463–1473, DOI: 10.3155/1047-3289.58.11.1463.

(8) Redington, A. L.; Derwent, R. G.; Witham, C. S.; Manning, A. J. Sensitivity of modelled sulphate and nitrate aerosol to cloud, pH and ammonia emissions. *Atmos. Environ.* **2009**, *43*, 3227–3234.

(9) Derwent, R.; Witham, C.; Redington, A.; Jenkin, M.; Stedman, J.; Yardley, R.; Hayman, G. Particulate matter at a rural location in southern England during 2006: Model sensitivities to precursor emissions. *Atmos. Environ.* **2009**, *43*, 689–696.

(10) Beer, R.; Shephard, M. W.; Kulawik, S. S.; Clough, S. A.; Eldering, A.; Bowman, K. W.; Sander, S. P.; Fisher, B. M.; Payne, V. H.; Luo, M. Z.; Osterman, G. B.; Worden, J. R. First satellite observations of lower tropospheric ammonia and methanol. *Geophys. Res. Lett.* **2008**, *35*, L09801, DOI: 10.1029/2008GL033642.

(11) Clarisse, L.; Clerbaux, C.; Dentener, F.; Hurtmans, D.; Coheur, P. F. Global ammonia distribution derived from infrared satellite observations. *Nat. Geosci.* **2009**, *2*, 479–483, DOI: 10.1038/ngeo551.

(12) Streets, D. G.; Bond, T. C.; Carmichael, G. R.; Fernandes, S. D.; Fu, Q.; He, D.; Klimont, Z.; Nelson, S. M.; Tsai, N. Y.; Wang, M. Q.; Woo, J. H.; Yarber, K. F. An inventory of gaseous and primary aerosol emissions in Asia in the year 2000. *J. Geophys. Res.* **2003**, *108*, 8809, DOI: 10.1029/2002JD003093.

(13) Wang, S. W.; Liao, Q. J. H.; Hu, Y. T.; Yan, X. Y. A Preliminary Inventory of NH3-N Emission and Its Temporal and Spatial Distribution of China. *Chin. J. Agro-Environ. Sci.* **2009**, *28* (3), 619–629.

(14) Dong, W. X.; Xing, J.; Wang, S. X. Temporal and Spatial Distribution of Anthropogenic Ammonia Emissions in China: 1994—2006. *Chin. J. Environ. Sci.* **2010**, *31* (7), 1457–1463.

(15) Zhao, D.; Wang, A. Emission of anthropogenic ammonia emission in Asia. *Atmos. Environ.* **1994**, *28*, 689–694.

(16) Yamaji, K.; Ohara, T.; Akimoto, H. Regional-specific emission inventory for NH_3, N_2O, and CH_4 via animal farming in South, Southeast, and East Asia. *Atmos. Environ.* **2004**, *38*, 7111–7121.

(17) Lu, Z.; Streets, D. G.; Zhang, Q.; Wang, S.; Carmichael, G. R.; Cheng, Y. F.; Wei, C.; Chin, M.; Diehl, T.; Tan, Q. Sulfur dioxide emissions in China and sulfur trends in East Asia since 2000. *Atmos. Chem. Phys.* **2010**, *10*, 6311–6331.

(18) Xing, J.; Wang, S. X.; Chatani, S.; Zhang, C. Y.; Wei, W.; Klimont, Z.; Cofala, J.; Amann, M.; Hao, J. M. Projections of Air Pollutant Emissions and its Impacts on Regional Air Quality in China in 2020. *Atmos. Chem. Phys.* **2011**, *11*, 3119–3136, DOI: 10.5194/acp-11-3119-2011.

(19) West, J. J.; Ansari, A. S.; Pandis, S. N. Marginal $PM_{2.5}$: Nonlinear aerosol mass response to sulfate reductions in the eastern United States. *J. Air Waste Manage. Assoc.* **1999**, *49*, 1415–1424.

(20) Zhao, Y.; Duan, L.; Xing, J.; Larssen, T.; Nielsen, C. P.; Hao, J. M. Soil Acidification in China: Is Controlling SO_2 Emissions Enough? *Environ. Sci. Technol.* **2009**, *43*, 8021–8026.

(21) Amann, M.; Bertok, I.; Borken, J.; Chambers, A.; Cofala, J.; Dentener, F.; Heyes, C.; Hoglund, L.; Klimont, Z.; Purohit, P.; Rafaj, P.; Schöpp, W.; Toth, G.; Wagner, F.; Winiwarter, W. *A Tool to Combat Air Pollution and Climate Change Simultaneously*; Methodology report; International Institute for Applied Systems Analysis (IIASA): Laxenburg, Austria, 2008.

(22) Klimont, Z.; Cofala, J.; Xing, J.; Wei, W.; Zhang, C.; Wang, S.; Kejun, J.; Bhandari, P.; Mathur, R.; Purohit, P.; Rafaj, P.; Chambers, A.; Amann, M. Projections of SO_2, NO_x and carbonaceous aerosols emissions in Asia. *Tellus, Ser. B* **2009**, *61*, 602–617.

(23) Zhang, M. S.; Luan, S. J. Application of NARSES in Evaluation of Ammonia Emission from Nitrogen Fertilizer Application in Planting System in China. *Chin. J. Anhui Agric. Sci.* **2009**, *37* (8), 3583–3586.

(24) Cao, G. L.; An, X. Q.; Zhou, C. H.; Ren, Y. Q.; Tu, J. Emission inventory of air pollutants in China. *Chin. Environ. Sci.* **2010**, *30* (7), 900–906.

(25) Byun, D. W.; Schere, L. K. Review of the governing equations, computational algorithms and other components of the models-3 Community Multiscale Air Quality (CMAQ) Modeling System. *Appl. Mech. Rev.* **2006**, *59* (2), 51–77.

(26) Zhang, M.; Uno, I.; Zhang, R.; Han, Z.; Wang, Z.; Pu, Y. Evaluation of the Models-3 Community Multi-scale Air Quality (CMAQ) modeling system with observations obtained during the TRACE-P experiment: comparison of ozone and its related species. *Atmos. Environ.* **2006**, *40* (26), 4874–4882.

(27) Streets, D. G.; Fu, J. S.; Jang, C.; Hao, J.; He, K.; Tang, X.; Zhang, Y.; Li, Z.; Zhang, Q.; Wang, L.; Wang, B.; Yu, C. Air quality during the 2008 Beijing Olympic games. *Atmos. Environ.* **2007**, *41* (3), 480–492.

(28) Fu, J. S.; Jang, C. J.; Streets, D. G.; Li, Z.; Kwok, R.; Park, R.; Hang, Z. MICS-Asia II: Evaluating gaseous pollutants in East Asia using an advanced modeling system: Models-3/CMAQ System. *Atmos. Environ.* **2008**, *42* (15), 3571–3583.

(29) Fu, J. S.; Streets, D. G.; Jang, C. J.; Hao, J.; He, K.; Wang, L.; Zhang, Q. Modeling Regional/Urban Ozone and Particulate Matter in Beijing, China. *J. Air Waste Manage. Assoc.* **2009**, *59*, 37–44.

(30) Wang, L.; Carey, C. J.; Zhang, Y.; Wang, K.; Zhang, Q.; Streets, D. G.; Fu, J.; Lei, Y.; Schreifels, J.; He, K.; Hao, J.; Lam, Y. F.; Lin, J.; Meskhidze, N.; Voorhees, S.; Evarts, D.; Phillips, S. Assessment of air quality benefits from national air pollution control policies in China. Part II: Evaluation of air quality predictions and air quality benefits assessment. *Atmos. Environ.* **2010**, *44*, 3449–3457.

(31) Li, L.; Chen, C. H.; Fu, J. S.; Huang, C.; Streets, D. G.; Huang, H. Y.; Zhang, G. F.; Wang, Y. J.; Jang, C. J.; Wang, H. L.; Chen, Y. R.; Fu, J. M. Air quality and emissions in the Yangtze River Delta, China. *Atmos. Chem. Phys.* **2011**, *11*, 1621–1639.

(32) U.S. Environmental Protection Agency. *Technical Support Document for the Proposed PM NAAQS Rule: Response Surface Modeling*; Office of Air Quality Planning and Standards: Research Triangle Park, NC, 2006.

(33) Xing, J.; Wang, S. X.; Jang, C.; Zhu, Y.; Hao, J. M. Nonlinear Response of Ozone to Precursor Emission Changes in China: a Modeling Study using Response Surface Methodology. *Atmos. Chem. Phys.* **2011**, *11*, 5027–5044, DOI: 10.5194/acp-11-5027-2011.

(34) Santner, T. J.; Williams, B. J.; Notz, W. *The Design and Analysis of Computer Experiments*; Springer Verlag: New York, 2003.

(35) Yarwood, G.; Wilson, G.; Morris, R. Development of The CAMx Particulate Source Apportionment Technology (Psat), final report; ENVIRON International Corporation, 2005.

(36) Koo, B.; Wilson, G. M.; Morris, R. E.; Dunker, A. M.; Yarwood, G. Comparison of Source Apportionment and Sensitivity Analysis in a Particulate Matter Air Quality Model. *Environ. Sci. Technol.* **2009**, *43*, 6669–6675.

(37) Chan, C. K.; Yao, X. H. Air pollution in mega cities in China. *Atmos. Environ.* **2008**, *42*, 1–42.

(38) Seinfeld, J. H.; Pandis, S. N. *Atmospheric Chemistry and Physics: From Air Pollution to Climate Change*; John Wiley and Sons, Inc.: New York, 2006.

(39) Zhang, Y.; Wen, X. Y.; Wang, K.; Vijayaraghavan, K.; Jacobson, M. Z. Probing into Regional O_3 and PM Pollution in the U.S., Part II. An Examination of Formation Mechanisms through a Process Analysis Technique and Sensitivity Study. *J. Geophys. Res.* **2009**, 114(D22305), DOI: 10.1029/2009JD011900.

(40) Blanchard, C. L.; Roth, P. M.; Tanenbaum, S. J.; Ziman, S. D.; Seinfeld, J. H. The use of ambient measurements to identify which precursor species limit aerosol formation. *J. Air Waste Manage. Assoc.* **2000**, *50*, 2073–2084.

(41) Makar, P. A.; Moran, M. D.; Zheng, Q.; Cousineau, S.; Sassi, M.; Duhamel, A.; Besner, M.; Davignon, D.; Crevier, L.-P.; Bouchet, V. S. Modelling the impacts of ammonia emissions reductions on North American air quality. *Atmos. Chem. Phys.* **2009**, *9*, 7183–7212, DOI: 10.5194/acp-9-7183-2009.